



Research Article

Numerical Investigation of Ribs Number Effect on Heat Transfer Inside A Heated Duct

Ahmed Rahmah Al-darraj¹, , Foad Faraji^{2,*}, 

¹ School of Engineering and Natural Sciences, Altinbas University, Istanbul-Turkey.

² School of Computing, Engineering & Digital Technologies Teesside University, UK

ARTICLE INFO

Article History

Received 20 Feb 2024

Revised: 19 Mar 2024

Accepted 21 Apr 2024

Published 19 May 2024

Keywords

Heated duct

ribs

turbulators

turbulence augment

vortex generators



ABSTRACT

Numerical simulations of flow and heat transfer are conducted in a three-dimensional square duct, including circular ribs positioned at the mid-height. The properties of the rib are examined, including the rib count (1-2-5-7) and the placement angle (0, 30, 45 degrees). Reynolds number is set as constant at 5000 for all studied cases. The existence of these ribs significantly influences heat transfer. The heat transfer rate is directly related to the quantity of ribs and positioning angle. The maximum recorded enhancement in Nusselt number is 30%.

1. INTRODUCTION

The enactment of heat transfer refers to any technique designed to augment the efficiency of a thermal system or elevate the heat transfer coefficient via various methodologies. The strategy for improving heat transfer has undergone substantial and swift advancement in recent years, as it is essential for conserving fossil fuels, a critical global objective due to its influence on decreasing carbon dioxide emissions and, thereby, alleviating the greenhouse effect. Furthermore, the worldwide increase in energy consumption correlates with population expansion [1-3]. Moreover, industrial and technological applications need the development of heat exchangers that are smaller and more lightweight but capable of high heat load, especially in the production of cooling systems for automobiles and spacecraft. This leads to material savings and, therefore, a cost reduction [4-5]. As a result, many efforts have been made for over a century to discover effective and cost-efficient enhancement methods that provide the aforementioned benefits. The generation of turbulence is an effective method for augmenting heat transfer, as it mitigates turbulent flow separation by inducing turbulence, thereby enhancing fluid mixing and impingement flows, which significantly boosts heat and momentum transfer [6-7].

Numerous researchers have investigated heat transfer enhancement inside ducts and tubes by different turbulence-inducing methods, including ribs and baffles. Ahmed [8] conducted an empirical and numerical study to investigate the heat transfer inside a pipe in the presence of different shapes of vortex generators, including rectangular, triangular, winglet, trapezoidal, and elliptical. The range of tested Reynolds numbers is (7200 -14400). The average heat transfer is found to be improved by 4-15% using winglet vortex generators. L. Wange and B. Sunden [9] analyzed thermal characteristics, both locally and averaged, for turbulent flow characterized by Reynolds numbers between 8,000 and 20,000 in a square duct, including a single heat-fluxed wall. Four rib configurations, including square, triangular, equilateral, and trapezoidal, with both decreasing and increasing height in the flow direction, are repetitively and orthogonally positioned on the heated wall, maintaining a constant rib blockage ratio (BR) of 0.1 while varying the rib pitch-to-height ratio (P/e) from 8 to 15. The results showed that the trapezoidal rib produces the highest Nusselt number and friction factor. Chunhua Min et al. [10] conducted an experimental study on a modified version of a rectangular longitudinal vortex generator (LVG) created by truncating the four corners of a standard rectangular wing. They investigated the fluid flow behavior and heat transfer

*Corresponding author. FFaraji@tees.ac.uk

characteristics of this modified LVG when placed within a rectangular channel, comparing its performance to that of the conventional rectangular LVG. The findings demonstrate that the MRW has enhanced flow and thermal transfer characteristics relative to the RW. The heat transmission was enhanced by the strong longitudinal vortices generated by the presence of the LVGs. M. Henze and J. von Wolfersdorf [11] examined the longitudinal vortices generated by tetrahedral vortex generators. The vortices and associated heat transfer are contingent upon the characteristics of the entering flow. The heat transmission was influenced by the ratio of the VG height to the thickness of the hydrodynamic boundary layer. The highest VG exhibited the most substantial improvement in heat transfer. A distinct group of authors has used numerical simulations to investigate the augmentation of heat transfer. K. Yongsiri et al. [12] performed simulations to analyze the behavior of turbulent flow within a channel containing inclined detached ribs on the lower wall. The study examined a range of Reynolds numbers between 4000 and 24,000 and considered various rib attack angles (α), including 0° , 15° , 30° , 45° , 60° , 75° , 105° , 120° , 135° , 150° , and 165° . Simulation results revealed that ribs oriented at a 60° attack angle enhanced the heat transfer rate by a factor of 1.74 compared to a smooth channel and ribs without inclination. Patankar [13] indicated that heat transport in a channel with staggered baffles is enhanced by an increase in baffle height and a reduction in baffle spacing.

An examination of the literature indicates a need for further enhancement and evaluation of novel vortex generators in thermal systems, owing to the extensive use of heat exchangers and air ducts in industrial applications. This study numerically investigates the impact of circular ribs on the hydro-thermal performance inside a square duct.

2. PHYSICAL MODEL

The purpose of a solar still is to use solar energy to evaporate, and condense water from sources such as seawater or SolidWorks 2014 was used to construct the 3D flow domain geometry. Initially, 2D drawings are created, followed by the use of 3D tools to produce the whole geometry. The computational domain comprises three sections inside a square piece of 4 cm. The first section is the entry zone, measuring 40 cm in length (10Dh) to guarantee a fully established flow. The following area is the testing region. The top and bottom surfaces are subjected to a continuous heat flow. The ribs are positioned in this area. The last component is the exhaust zone, which links the test region to the surrounding environment. This zone protects the test area from environmental influences. Figures (1) and (2) illustrate the model in two-dimensional and three-dimensional representations.



Fig. 1. 2d- section of the model

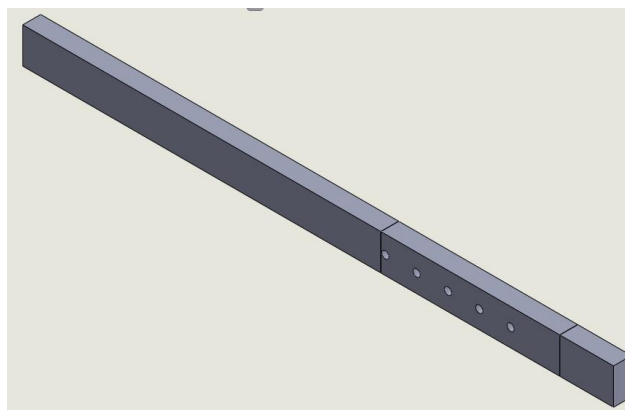


Fig. 2. The model

3. MESHING

The creation of a computational mesh involves partitioning the flow domain into minute components and then resolving the governing equations for these elements. Two volumetric meshing techniques were employed: structured and unstructured [14]. The structured meshing has components of approximately uniform dimensions. This kind is used with areas of uniform shape. The unstructured meshing has components of varying sizes and forms. This kind of meshing is often appropriate for intricate geometry. Due to the uniform cross-section of the entry and exhaust sectors, structured meshing is used to discretize these areas. Hexagonal elements are used to discretize these areas. The test area exhibits non-uniformity due to the rib's existence, necessitating an unstructured meshing approach. Tetrahedral components were used to create the mesh in this area.

The element number substantially influences the simulation results in this study. The element number is significant in the test zone, encompassing fluid movement and heat transfer. The grid consists of a total of 1,420,557 components. This figure was established by evaluating the impact of the element count on the average heat transfer coefficient at the test surface. This test is shown in Table 1. The meshed domain is seen in Figure 3.

TABLE I. VARIATION OF AVERAGE HEAT TRANSFER COEFFICIENT WITH ELEMENTS NUMBER.

| Elements number | h_{av} |
|-----------------|----------|
| 389571 | 18 |
| 569127 | 21 |
| 866432 | 23 |
| 1150000 | 24 |
| 1420577 | 24.36 |

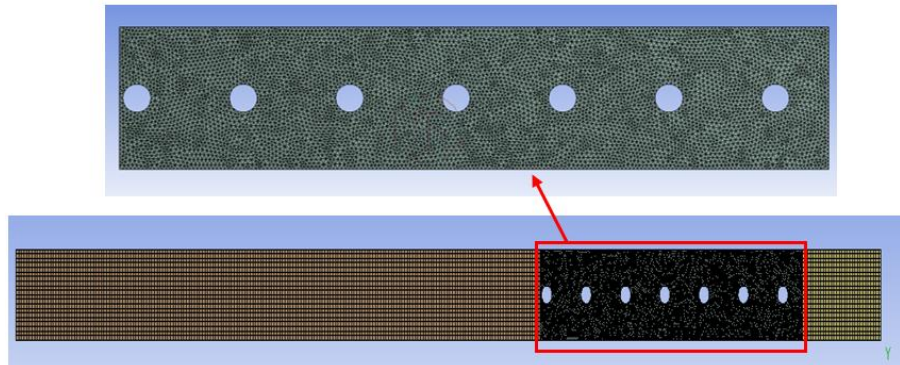


Fig. 3. The meshed domain

4. GOVERNING EQUATIONS

The Navier-Stokes equations, expressed in tensor notation, decompose variables into mean and fluctuation components through Reynolds averaging. This process resembles velocity decomposition [15]:

$$u_i = \bar{u}_i + u'_i \quad (1)$$

Where \mathbf{u}_i is the instantaneous fluid velocity, \mathbf{u}'_i is the velocity fluctuation and $\bar{\mathbf{u}}_i$ is the time-averaged value of \mathbf{u}_i at a point.

4.1 Continuity Equation

This equation defines the law of conservation of mass, which asserts that the mass of a steady-state system The continuity equation delineates the principle of mass conservation, asserting that the mass of a steady-state system remains invariant across time.

$$\frac{\partial \rho u}{\partial x} + \frac{\partial \rho v}{\partial y} + \frac{\partial \rho w}{\partial z} = 0 \quad (2)$$

The above equation may be expressed as follows, given that the mass density of fluid remains constant:

$$\frac{\partial u}{\partial x} + \frac{\partial v}{\partial x} + \frac{\partial w}{\partial x} = 0 \quad (3)$$

Then, the continuity equation is stated as:

$$\frac{\partial u_i}{\partial x_i} = 0 \quad (4)$$

4.2 Momentum Equation

The concept of conservation of momentum asserts that in an isolated system, the total momentum remains constant before and after a collision between objects. The lost momentum is equivalent to the gain. The momentum equation is expressed as [15]:

$$\rho \frac{\partial u_i u_j}{\partial x_j} = -\frac{\partial P}{\partial x_i} + \mu \frac{\partial}{\partial x_j} \left(\frac{\partial u_i}{\partial x_j} + \frac{\partial u_j}{\partial x_i} \right) + \rho \frac{\partial}{\partial x_j} (-\overline{u_i' u_j'}) \quad (5)$$

4.3 Energy Equation

The law of energy conservation states that the total energy within an isolated system remains constant over time. The energy equation can be articulated as follows [15]:

$$\rho c_p \frac{\partial u_i T}{\partial x_i} = \frac{\partial}{\partial x_i} \left(\lambda \frac{\partial T}{\partial x_i} - \rho \overline{u_i' T'} \right) \quad (6)$$

Where λ is thermal conductivity

4.4 Turbulence Model

Numerous turbulence models in Fluent are available to simulate diverse flow scenarios. The K- ϵ realizable model was used in this study. This model is advised [16] for flows characterized by vortices and rotation, such as those occurring inside ducts, including ribs.

5. BOUNDARY CONDITIONS

The Governing equations are solved by utilizing the following boundary conditions as in Figure (4):

- Left face: velocity inlet
- Right face: pressure outlet.
- Upper and lower face of test section: heat flux

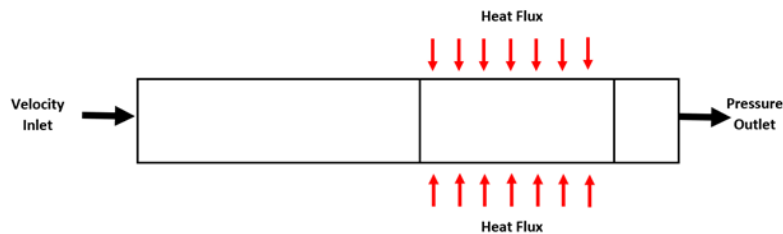


Fig. 4. The Boundary conditions

5. SOLUTION

In order to perform numerical simulations of the natural convection inside the annulus and between the glass cover and the surroundings, the ANSYS Fluent set-up, in detail described below, was chosen according to ANSYS recommendation [14]. The spatial discretization settings used for numerical simulations are the second order for all equations. The convergence criteria are set to 10^{-5} for all equations.

6. RESULTS

This study quantitatively examined heat transfer and flow structure inside a square duct, including circular ribs. This study analyzes the impact of the number of ribs (1, 2, 5, 7) and the placement angle θ (0, 30, 45 degrees). The ratio of rib height to duct height is 0.2. The convective heat transfer coefficient is calculated on the test section's top face. The average Nusselt number is then derived from the mean heat transfer coefficient.

6.1 Effect of Ribs Number

Figure (5) illustrates a relationship between the local heat transfer coefficient and the number of ribs inside the test section. The graphic demonstrates an improvement in the heat transfer coefficient as the number of ribs increases up to a particular threshold. This improvement is attributable to heightened turbulence levels. The number of ribs significantly influences pressure. As the number increases, further fluid is impeded, resulting in an elevated pressure decrease, as seen in Figure (6). Figure (7) illustrates the increase in the average Nusselt number for various rib configurations in comparison to the smooth duct. The improvement may reach 30%.

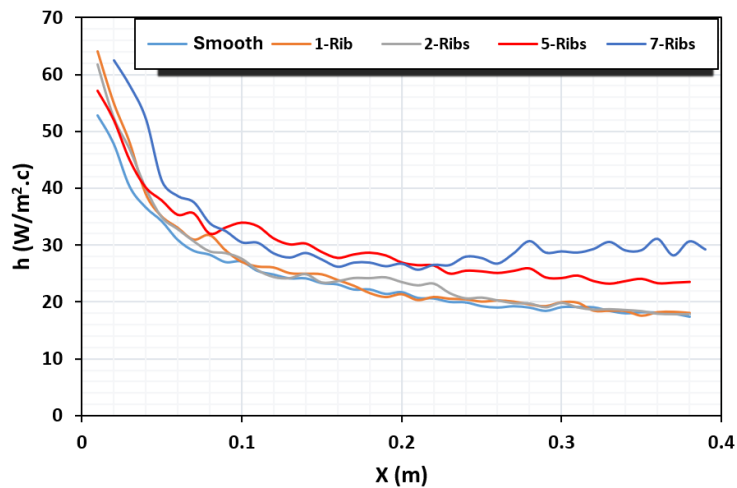


Fig. 5. Local heat transfer coefficient for different ribs number

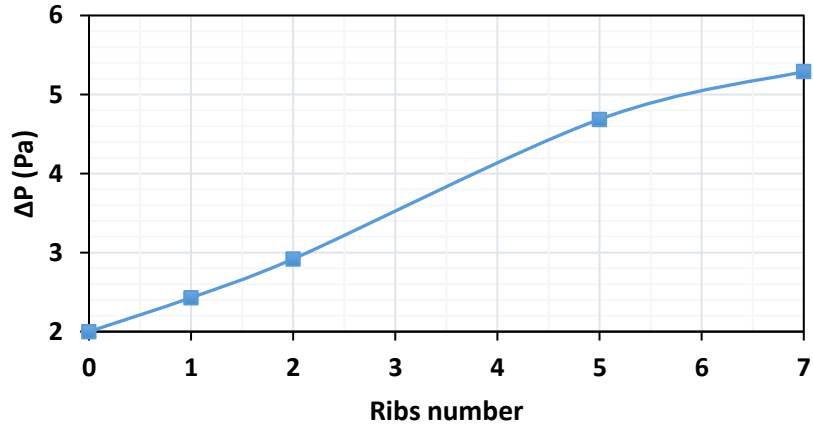


Fig. 6. Effect of ribs number on pressure drop.

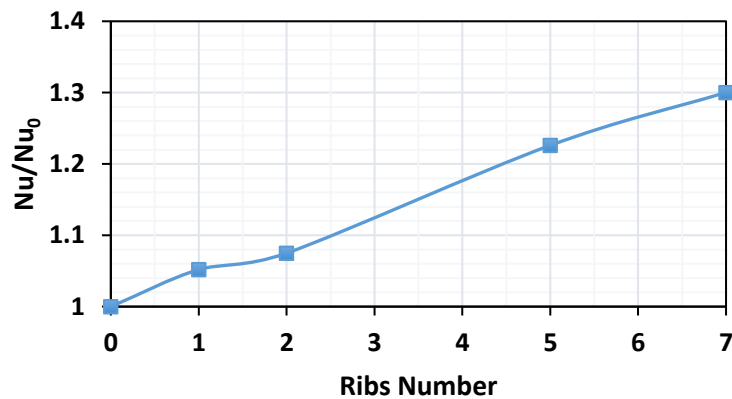


Fig. 7. Enhancement of average Nusselt number.

6.2 Effect of Placement Angle

Figure (8) illustrates the influence of the rib placing angle on local heat transfer at a velocity of $V=2\text{m/s}$ with three ribs present. Heat transfer escalates with an increase in angle owing to the enhancement of the turbulence zone. Figure (9) illustrates the impact of the angle on pressure drop. Figure (10) illustrates the increase in the average Nusselt number resulting from this angle's influence. Nusselt number was increased by 6%.

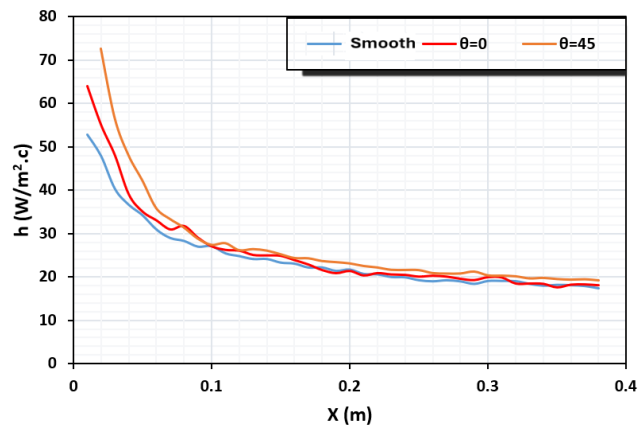


Fig. 8. Local heat transfer coefficient for different angles.

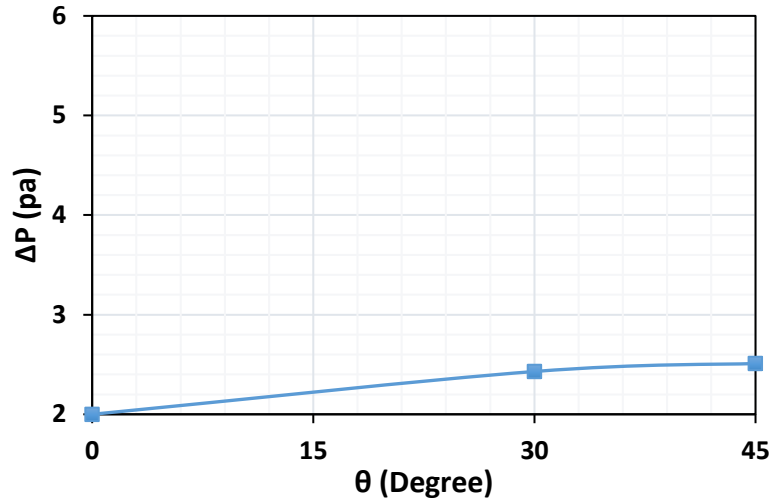


Fig. 9. Pressure drop.

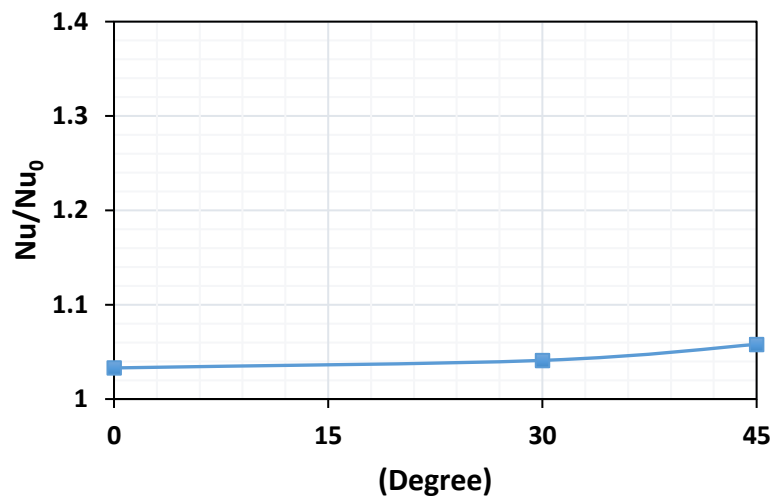


Fig. 10. Enhancement of average Nusselt number.

6. CONCLUSIONS

This research investigated numerically the heat transfer and pressure drop characteristics in a heated square duct, including circular ribs (vortex generators) positioned along the duct's centerline. The Reynolds number was maintained at 5000 throughout all scenarios, with ribs number of 1, 2, and 3 and rib placement angles (θ) of 0, 30, and 45 degrees. The subsequent findings are as follows:

1. Generally, ribs enhance heat transfer by increasing turbulence.
2. The number of ribs significantly influences heat transfer.
3. The placement angle positively affects heat transfer.
4. The maximum improvement is 30% for seven ribs.

Conflicts Of Interest

The author's paper explicitly states that there are no conflicts of interest to be disclosed.

Funding

The author's paper clearly indicates that the research was conducted without any funding from external sources.

Acknowledgment

The author acknowledges the institution for their commitment to fostering a research-oriented culture and providing a platform for knowledge dissemination.

References

- [1] F. Mallor, C. S. Vila, A. Ianiro, and S. Discetti, "Wall-mounted perforated cubes in a boundary layer: Local heat transfer enhancement and control," *Int. J. Heat Mass Transfer*, vol. 117, pp. 498–507, 2018.
- [2] F. Mallor, M. Raiola, C. S. Vila, R. Örlü, S. Discetti, and A. Ianiro, "Modal decomposition of flow fields and convective heat transfer maps: An application to wall-proximity square ribs," *Exp. Therm. Fluid Sci.*, vol. 102, pp. 517–527, 2019.
- [3] Z. Ke, C. L. Chen, K. Li, S. Wang, and C. H. Chen, "Vortex dynamics and heat transfer of longitudinal vortex generators in a rectangular channel," *Int. J. Heat Mass Transfer*, vol. 132, pp. 871–885, 2019.
- [4] N. Puzu, S. Prasertsan, and C. Nuntadusit, "Heat transfer enhancement and flow characteristics of vortex generating jet on a flat plate with turbulent boundary layer," *Appl. Therm. Eng.*, vol. 148, pp. 196–207, 2019.
- [5] B. Giachetti, M. Fénot, D. Couton, and F. Plourde, "Influence of Reynolds number synthetic jet dynamics in crossflow configuration on heat transfer enhancement," *Int. J. Heat Mass Transfer*, vol. 118, pp. 1–13, 2018.
- [6] M. J. Al-Dulaimi, F. A. Kareem, and F. A. Hamad, "Numerical investigation of the heat transfer enhancement inside a square duct with rectangular vortex generators," *J. Therm. Eng.*, vol. 8, pp. 1–13, 2022.
- [7] M. J. Al-Dulaimi, A. Abdulhadi, and A. Hamza, "Effect of circular turbulators on heat transfer in a square duct," *J. Mech. Eng. Res. Dev.*, vol. 44, pp. 217–229, 2021.
- [8] A. H. Yousif, "Enhancement of heat transfer from heated cylinder inside duct by using vortex generator," Ph.D. dissertation, Dept. Mech. Eng., Univ. Technol., Baghdad, Iraq, 2006.
- [9] L. Wange and B. Sunden, "Experimental investigation of local heat transfer in a square duct with various-shaped ribs," *Heat Mass Transfer*, vol. 43, pp. 759–766, 2007.
- [10] C. Min, C. Qi, X. Kong, and J. Dong, "Experimental study of rectangular channel with modified rectangular longitudinal vortex generators," *Int. J. Heat Mass Transfer*, vol. 53, no. 15-16, pp. 3023–3029, 2010.
- [11] M. Henze and J. von Wolfersdorff, "Flow and heat transfer characteristics behind vortex generators," *Int. J. Heat Fluid Flow*, vol. 32, no. 1, pp. 318–328, 2011.
- [12] K. Yongsiria, P. Eiamsa-ard, K. Wongchareec, and S. Eiamsa-ard, "Augmented heat transfer in a turbulent channel flow with inclined detached-ribs," *Case Studies Therm. Eng.*, vol. 3, pp. 1–10, 2014.
- [13] K. M. Kelkar and S. V. Patankar, "Numerical prediction of flow and heat transfer in a parallel plate channel with staggered fins," *J. Heat Transfer*, vol. 109, no. 1, pp. 25–30, 1987.
- [14] ANSYS Meshing Guide, 2016.
- [15] ANSYS Theory Guide, 2016.
- [16] S. Dogru, T. Tunay, and H. Zontul, "Effects of vortex generator aspect ratio on enhancement of heat transfer in a straight channel," in *Proc. 1st Int. Mediterranean Sci. Eng. Congr.*, 2016, pp. 3378–3386.